Extended-time multi-taper frequency domain cross-correlation receiver function estimation

George Helffrich
Earth Sciences, University of Bristol, Wills Mem. Bldg., Queen's Road, Bristol BS8 1RJ, UK

Manuscript for submission to *Bulletin of the Seismological Society of America*: 29 April 2005; revised 17 July 2005; accepted 29 August 2005.

Abstract. This note documents a method that successfully yields frequency domain cross-correlation receiver functions without amplitude loss at long time lags and without sacrificing any of the advantages of the method. After describing it, an analysis of synthetics of transition zone structure shows that the method provides a way to investigate mantle structure from the surface through the transition zone and deeper.

Introduction.

The receiver function method is a common analysis technique of great conceptual simplicity and widely used by seismologists. The method relies on the insight that the coda following a teleseismic body wave arrival largely consists of mode-converted energy emanating from the impedance contrasts arising from layering in the earth near the receiver (Phinney, 1964). As such, this mode-converted wave train is a convolution of the incident wave with the earth structure. Under the geologically reasonable approximation of horizontal layering (which later extensions to the method relax), deconvolving the vertical component of the P-wave arrival (an estimate of the incident wave) from the radial component (the mode-converted wave train) yields an estimate of the earth structure: a sequence of pulses in time produced by the incident wave field, also called

the receiver function. The concept is simple, but reliable implementation is difficult.

The implementation difficulties stem from the instability of deconvolution. This led to the use of a variety of stabilization methods in order to estimate the receiver function. They include frequency domain division with a spectral water level (Langston, 1979; Owens et al., 1983; Ammon, 1991), deconvolution in the time domain by least-squares estimation (Abers et al., 1995), iterative deconvolution in the time domain (Ligorría and Ammon, 1999), and multi-taper frequency domain cross-correlation receiver function (MTRF) (Park and Levin, 2000). Park and Levin (2000) compare and contrast the methods, to which I refer the reader interested in those issues. One key advantage of the MTRF is its resistance to noise, which recommends its use in environments such as ocean islands with high noise levels in the seismic band. This advantage is due to MTRF's use of multi-tapers to minimize spectral leakage and its frequency dependent downweighting of the noisy portions of the spectrum. A disadvantage of the Park and Levin (2000) MTRF method (P&L MTRF, hereafter) is that only the first 10 seconds or so of the receiver function contains a usable signal. The receiver function amplitude decays at longer lags, principally due to the short analysis windows (about 60 seconds, but extendable for some target time-bandwidth products) forced by the assumption inherent in the use of multiple tapers that the signal is stationary through the taper duration (Thomson, 1982; Park et al., 1987; Park and Levin, 2000; 2005). This defeats MTRF's direct use for transition zone structure studies, but there are remedies if one is willing to sacrifice continuity of the receiver function from zero to long lags (Park and Levin, 2005). Continuity, however, is a crucial factor if one wishes to migrate a collection of

receiver functions in a common conversion point gather to form vertical structure sections through the crust and mantle, as for example, in Dueker and Sheehan (1997).

This combination of attractive properties and drawbacks motivated a development effort to compute MTRFs in a way that preserves their amplitudes for arbitrarily long times. The description follows in the following paragraphs, plus, using deconvolved synthetics for transition zone structure, a demonstration of the method's ability to surmount the amplitude decay problem at long lags.

Method.

The method is akin to an overlap-and-sum technique for estimating stationary signal spectra in long time series (Press et al., 1992). Unlike overlap and sum spectral estimation, however, it preserves phase information by using a sequence of short multiple tapers to window the time series over its full length and to sum the individual Fourier-transformed (FT) signals into a frequency domain representation that preserves the phase lags for each subwindow of the time series. These ideas are sketched in Figure 1.

In practice, for data sampled at 20 Hz, three 2.5π prolate tapers of 10 seconds duration for windowing, with 50% window overlap works well. Each taper windows the data in the whole analysis segment after which the FT is calculated and summed with previous FTs for that taper. Following that, the standard methods for forming multi-taper spectral estimates (Thomson, 1982; Park et al., 1987) lead to a receiver function estimate $H_R(f)$ by calculating the cross-correlation of the radial (R) component with the vertical (Z) component Fourier transform, using the pre-arrival Z-component power as an estimate of the noise at a particular frequency for weighting, as do Park and Levin (2000):

$$H_R(f) = \frac{\sum_{k=1}^{K} (Y_Z^{(k)}(f))^* Y_R^{(k)}(f)}{S_0(f) + \sum_{k=1}^{K} (Y_Z^{(k)}(f))^* Y_Z^{(k)}(f)} \quad . \tag{1}$$

Here $Y_{R,Z}^{(k)}$ are the k-th of K Slepian-tapered Fourier transforms of the R- or Z-component signal, $S_0(f)$ is the spectrum estimate of the pre-event noise on the vertical component, and * represents complex conjugation. Applying a $\cos^2$ frequency domain taper implements a high-frequency cutoff to the receiver function. Along with the multiple windows, this leads to normalization factors for the spectra that read,

$$\underbrace{\frac{1}{N_{win}}}_{\text{multi-window}} \times \underbrace{\frac{N_{ft}}{N_{fc}}}_{\cos^2 \text{ window}} \times \underbrace{\frac{2}{N_{ft}}}_{\text{FFT normalization}} , \tag{2}$$

where N_{win} is the number of windows contributing to the sum, N_{ft} is the number of points in the FT, and N_{fc} is the number of nonzero points in the $\cos^2$ taper. Because the overlap is the same in every $Y_{R,Z}^{(k)}$, no explicit correction is needed for it. The result is a receiver function as long as the original analysis segment. A useful way to distinguish this from P&L MTRF would be to call it an extended-time MTRF, or ET MTRF.

Examples.

Figure 2 shows an example where a single unit impulse is deconvolved from a train of unit impulse functions spaced every 6 seconds from zero to 60 seconds. There are two items to note in the example. The first is that there is uniform amplitude though the analysis window, as compared to varying amplitude when a single tapering position is used. The second is that amplitudes vary mildly by about 2% through the receiver function. Both of these characteristics arise because the tapers are not uniformly sensitive to an impulse in the taper window. Recall that multi-tapers are designed for

spectral estimation of stationary signals (Thomson, 1982; Park et al., 1987); impulse functions are not of this category.

Figure 3 shows a reflectivity synthetic of a P-wave arrival from a 400 km deep source located at 60 degrees distance from a receiver, and the deconvolution of the vertical component from the radial. The reference model is SP6 (Morelli and Dziewonski, 1993), with discontinuities at 20 (intra-crustal), 35 (Moho), 210 (S only), 410 and 660 km depth. For comparison, we show the same seismograms deconvolved using Park and Levin's (2000) method with the same analysis window. Agreement in the initial portions of the traces is excellent. The ET MTRF function additionally features prominent arrivals from the P-to-S conversions at 410 and 660 km depth at ~44 s and ~68 s. However, it also contains a complete record of the crustal structure as well, with middle-crust and Moho conversions at ~2.5 and ~4 seconds, and their reverberations.

Conclusion.

The purpose of this note is to introduce the ET MTRF and to demonstrate the viability of using multi-taper cross correlation estimation of receiver functions without requiring short analysis windows. The method described here is capable of being used for receiver function investigations where estimates at long lags are required, in, for example, transition zone structure investigations.

Acknowledgements. I thank Jeff Park for a preprint, discussions about the method, and for code to calculate the P&L MTRF.

Figure 1

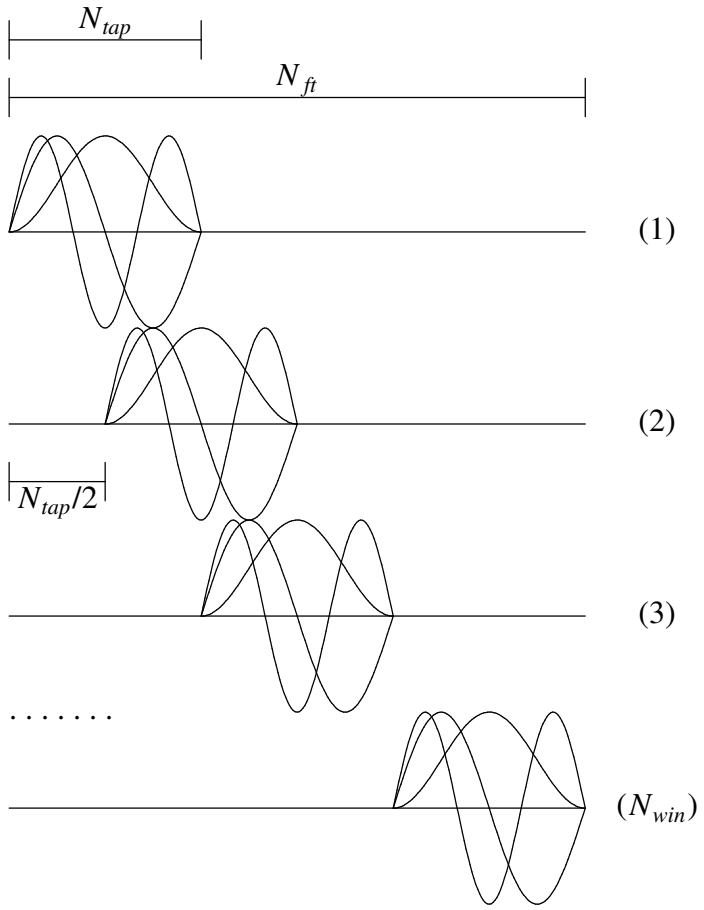

Sketch of construction method for K=3 Slepian tapers. The duration of the analysis segment is given by the N_{ft} points indicated by the top bar. The multiple tapers select each windowing interval of N_{tap} points, and a full N_{ft} point FT is taken of the whole analysis segment and accumulated N_{win} times for each tapered trace FT $Y^{(k)}(f)$, $k = 1, \cdots, K$. The K individual taper spectra are combined in the standard way for leakage resistance.

Figure 2

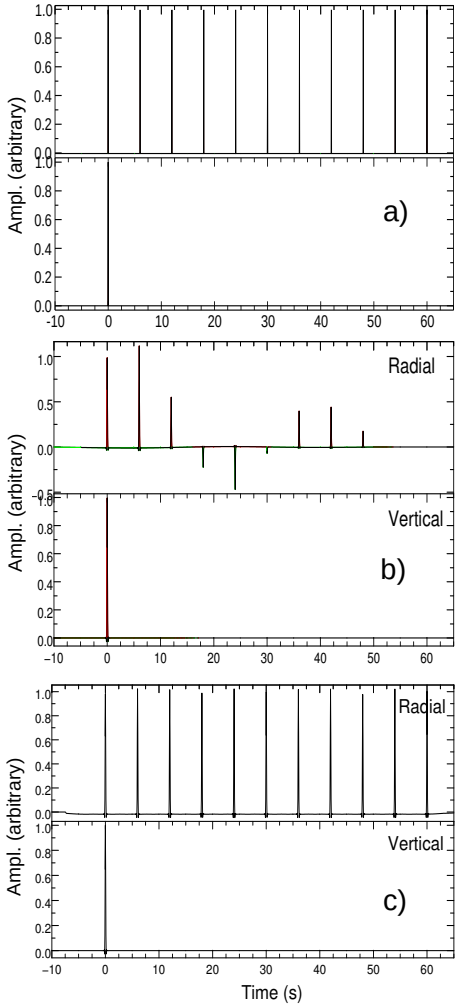

Example of a string of unit impulse functions deconvolved with single unit impulse. Sampling rate is 20 Hz and the deconvolution frequency cutoff is 8 Hz. a) Synthetic impulse string and single unit impulse deconvolved from the impulse string. b) P&L MTRF deconvolution. The measurement window starts 10 s before the first impulse and extends to 50 s after it. c) ET MTRF deconvolution. The measurement window starts 5 s before the first impulse and extends to 65 s after it. Note non-constancy of amplitude through measurement window in P&L MTRF as compared to approximately constant amplitude ±2% for ET MTRF.

Figure 3

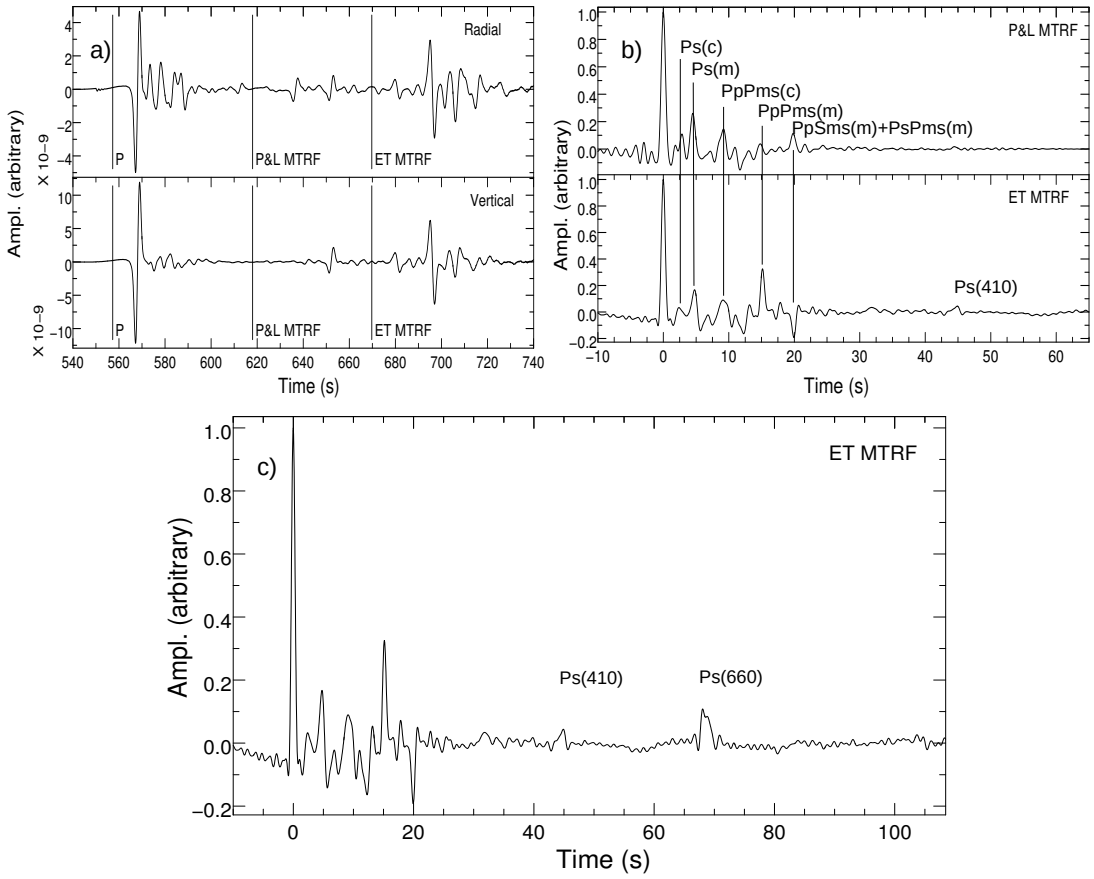

Example of reflectivity velocity seismogram using the SP6 model with source at 60° distance and 400 km depth, deconvolved using the ET MTRF and P&L MTRF. a) Top panels indicate radial and vertical synthetic seismograms. Vertical lines mark beginning and end of measurement windows for the P&L and ET MTRFs; both start at the P marker. b) Estimated radial receiver function using the P&L and ET MTRFs. Frequency cutoff is 1.5 Hz. Note that P&L MTRF amplitude drops after 10 s, whereas the ET MTRF amplitude is sustained out to the end of the window. Crustal and mantle Ps conversions and reverberations marked (c - intracrustal discontinuity at 20 km, m - Moho at 35 km). c) ET MTRF for whole measurement

interval shown in (a). Note preservation of shallow structure and reverberations between 0-20 s, as well as the prominent arrivals from 410 and 660 km depth at 44 and 67 s. Mild undulation is due to low frequency numerical noise in synthetic.

REFERENCES

Abers, G. A., X. Hu, and L. R. Sykes (1995). Source scaling of earthquakes in the Shumagin region, Alaska: Time-domain inversions of regional waveforms, *Geophys. J. Int.,* **123,** 41-58.

Ammon, C. J. (1991). The isolation of receiver effects from teleseismic P waveforms, *Bull. Seismol. Soc. Am.,* **81,** 2504-2510.

Dueker, K. D. and A. F. Sheehan (1997). Mantle discontinuity structure from midpoint stacks of converted P to S waves across the Yellowstone hotspot track, *J. Geophys. Res.,* **102,** 8313-8327.

Langston, C. A. (1979). Structure under Mount Rainier, Washington, inferred from teleseismic body waves, *J. Geophys. Res.,* **84,** 4749-4762.

Ligorría, J. P. and C. J. Ammon (1999). Iterative deconvolution and receiver-function estimation, *Bull. Seismol. Soc. Am.,* **89,** 1395-1400.

Morelli, A. and A. M. Dziewonski (1993). Body wave traveltimes and a spherically symmetric P- and S-wave velocity model, *Geophys. J. Int.,* **112,** 178-194.

Owens, T. J., S. R. Taylor, and G. Zandt (1983). Isolation and enhancement of the response of local seismic structure from teleseismic P-waveforms, *Lawrence Livermore Lab. Report UCID 19809,* 1-33.

Park, J. and V. Levin (2000). Receiver functions from multiple-taper spectral correlation

estimates, *Bull. Seismol. Soc. Am.,* **90,** 1507-1520.

Park, J. and V. Levin (2005). Receiver functions from multiple-taper spectral correlation: Statistics, single-station migration, and jackknife uncertainty, *Geophys. J. Int.,* **(submitted).**

Park, J., C. R. Lindberg, and F. L. Vernon, III (1987). Multitaper analysis of high-frequency seismograms, *J. Geophys. Res.,* **92,** 12675-12684.

Phinney, R. A. (1964). Structure of earths crust from spectral behavior of long-period body waves, *J. Geophys. Res.,* **69,** 2997-3017.

Press, W. H., S. A. Teukolsky, W. T. Vetterling, and B. P. Flannery (1992). *Numerical Recipes (2nd ed.),* Cambridge University Press, Cambridge, UK, xxvi+963pp.

Thomson, D. J. (1982). Spectrum estimation and harmonic analysis, *IEEE Proc.,* **70,** 1055-1096.